Original Article

MOLECULAR DYNAMICS GUIDED 4D QSAR STUDIES ON CHROMENONE BASED DNA-DEPENDENT PROTEIN KINASE INHIBITORS

RAJESH B. PATIL*, SANJAY D. SAWANT, RAKHI R. TIKHE

Sinhgad Technical Education Society's, Smt. Kashibai Navale College of Pharmacy, Pune-Saswad Road, Kondhwa (Bk), Pune 411048, Maharashtra, India.
Email: rajshama1@yahoo.com

ABSTRACT

Objective: Developing 4D QSAR model for chromenones as DNA-protein kinase inhibitors with LQTAgrid program and MATLAB with PLS Tool box.

Methods: 2D structures of forty five chromenones and pyrimido [2,1-a] isoquinolin-4-ones were drawn in Marvin application and subsequently converted to 3D format. With PRODRG server coordinate and topology files were generated. Molecular dynamics simulation for 20 ps was carried out in Gromacs4.6.3. Conformation ensemble for each molecule was aligned with the most active compound 22. Interaction energy descriptors were computed by placing NH_3^+ probe with LQTA grid program. 4D QSAR model was built-in MATLAB workspace with PLS Toolbox.

Results: 4D QSAR model developed with PLS regression showed root mean square error 0.188741, root mean square error predicted 0.575649, prediction bias -0.0221941, R^2 calculated for training set 0.834502. The model built could predict the DNA-PK inhibitory activity for analogous compounds with reasonably good predictive ability. The Leenard Jones interaction descriptors were found important in the model suggesting the importance of 3D steric features in the molecule. These facts could be exploited in designing newer DNK-PK inhibitors with improved activity.

Conclusion: 4D QSAR model was developed with good squared correlation coefficient of 0.834502. Few Leenard Jones descriptors were found contributing to the model. The 4D QSAR model could be used in designing more active DNK-PK inhibitors.

Keywords: Chromenones, 4D QSAR, DNA-Protein kinase inhibitors, LQTA grid, MATLAB, PLS regression.

INTRODUCTION

Chromenones are important class of bioactive molecules consisting of chromen-2-ones and chromen-4-ones. The flavones, isoflavones, flavanoids and coumarins have been extensively studied phyto constituents belonging to chromen-2-ones and chromen-4-ones class. Chromenones derivatives possess diverse pharmacological activities including antitumor [1, 2], antivascular [3], antimicrobial [4, 5], antioxidant [6], TNF-a inhibitor [7], antifungal [8], anticoagulant[9], anti spasmolytic [10, 11], estrogenic [12, 13], antiviral[14], anthelminthic [15], anti-HIV [16], antitubercular [17, 18], anti-inflammatory [19, 20], herbicidal [21], analgesic [22] and anticonvulsant [23, 24] activity. Wortmannin and LY294002 (1) (fig. 1) are the benchmark phosphatidylinositol 3-kinase (PI 3-K) inhibitors and inhibit other kinases from PI 3-K family *viz.* DNA-dependent protein kinase (DNA-PK).

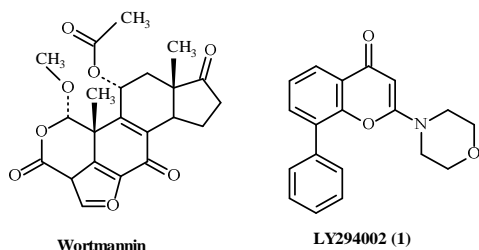**Wortmannin**   **LY294002 (1)**

Fig. 1: PI 3-K inhibitors

The survival of cancer cell against radio or chemotherapy due to their ability to repair DNA damage has been concerned in development of anticancer agents. DNK-PK, serine/threonine protein kinase, is the key enzyme in repair of DNA double strand break and has homology in the kinase domain of PI 3-K family. Griffin RJ *et al* [25] reported chromenones and pyrimido[2,1-a]isoquinolin-4-ones as DNA-PK inhibitors. This report highlights the importance of morpholine ring, presence of fused benzene ring

at 6, 7 and 7, 8 positions and carbonyl oxygen of chromenone. Quantitative structure activity relationship (QSAR) studies have been an important strategy in drug design [26]. Since its inception, QSAR approaches have evolved from 2D QSAR to more complex 4D QSAR. A 4D QSAR approach proposed by Hopfinger and co-workers [27] exploits conformational flexibility of ligand and freedom of alignment in three-dimensional spaces as required in 3D QSAR. In this approach grid cell occupancy descriptors, GCODs are calculated by aligning the set of molecules in the defined grid box. GOCDs are good measure of interaction pharmacophore elements, IPEs for atom sets like polar positive, polar negative, aromatic, hydrogen bond acceptor, hydrogen bond donor. The 4D QSAR models built with this formalism can be a way of designing bioactive molecules. In a pursuit of designing newer DNA-PK and PI 3-K inhibitors, 4D-QSAR study was carried out on the chromenones and pyrimido[2,1-a]isoquinolin-4-ones from the literature [25] with 4D QSAR approach called LQTAgrid-QSAR [28] (LQTA, Theoretical and Applied Chemometrics Laboratory, State University of Campinas, Brazil). Manuscript presents the 4D QSAR methodology and model built with Partial Least Squares (PLS) chemometric method.

MATERIAL AND METHODS

Computer hardware and software

Computational work was carried out on Ubuntu 12.0 and windows XP operating system. Software used included Autodock 4.2 with mgltools 1.5.6 [29], Marvin Sketch, UCSF Chimera1.8rc, Discovery Studio 3.5 (Biova, Inc.), MATLAB 7.7.0 (R2008b) (MathWorks, Inc.), PLS Toolbox version 7.51 (Eigenvector Research, Inc), Pymol version1.3 (from Schrodinger, LLC), LQTAgrid (Martins JPA et al., 2009) and Gromacs 4.6.3 (a molecular dynamics suite) [30].
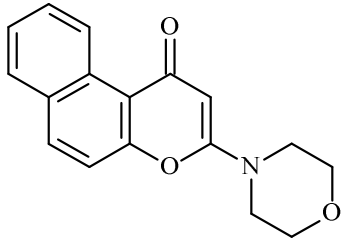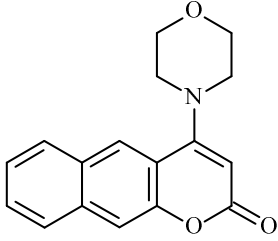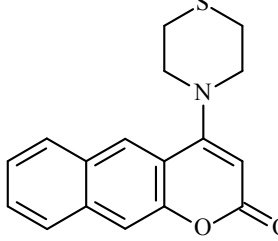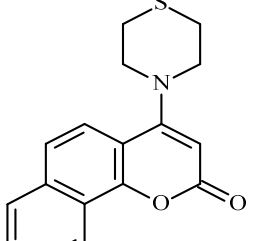
Dataset

Forty-five compounds presented in table 1 have been taken from the report of Griffin RJ *et al* [25]. Based on the substitution pattern in these derivatives 11 compounds were selected as test set and remaining 34 compounds as training set. DNA-PK IC50 in μM was transformed to pIC50 by taking the negative logarithm of IC50 values in moles.

Table 1: Structures of compounds
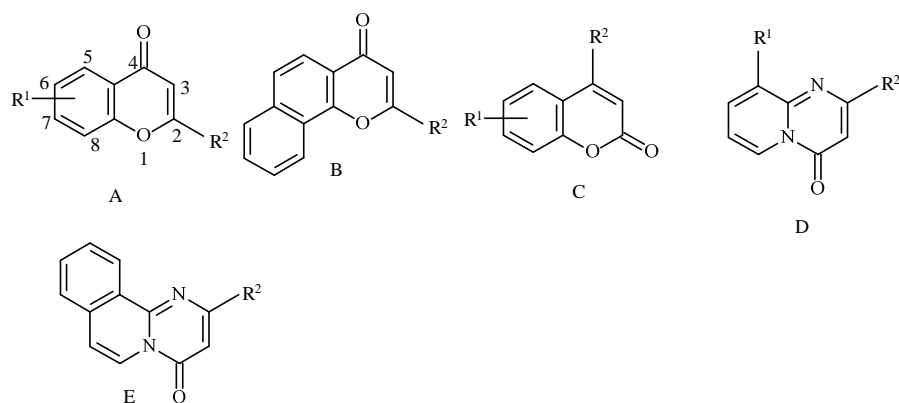
Compound No.	General structure	R¹	R²	pIC50 (mole)
1	A	8-Phenyl	(morpholine)	5.832683
2	B	-	(morpholine)	6.638272
3				6.585027
4				5.860121
5*				6.443697
6				6.408935

No.				Value
7				5.90309
8				5.489455
9				5.288193
10*				5.176526
11				5.721246
12*	E	-	—N(morpholine)	6.552842
13	A	H	—N(morpholine)	5.899629
14*	A	8-CH$_3$	—N(morpholine)	5.782516
15	A	7-OCH$_3$	—N(morpholine)	6.022276
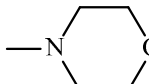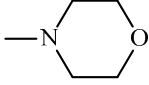
16*	A	8-OCH$_3$		5.920819
17	A	6-Phenyl		5.649752
18	A	8-Phenyl		5.330683
19	A	8-Phenyl		5.793174
20	B	-		5.496209
21*	B	-		5.03292
22	B	-		6.721246
23	B	-		5.383
24	B	-		5.453457
25	C	H		5.316953
26*	C	H		5.055024
27	C	6-CH$_3$		5.271646
28	C	8-CH$_3$		5.094204
29	C	6-OCH$_3$		5.756962
30	C	7-OCH$_3$		4.946537
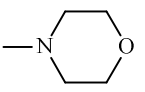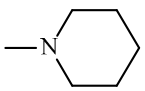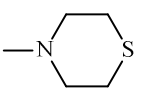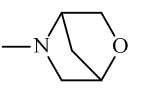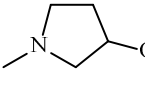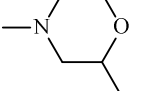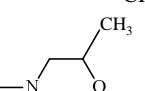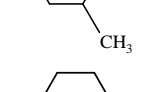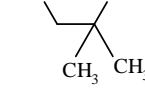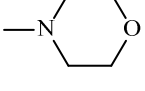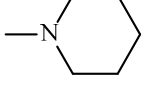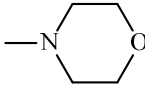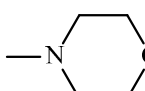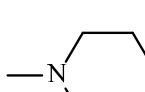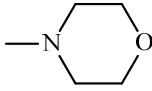
31*	C	8-OCH$_3$		4.960983
32	C	6-Cl		5.485452
33*	B	-	Phenyl	5.302771
34	B	-		5.066007
35	B	-		5.243364
36	B	-		5.716699
37*	D	H		5.69897
38	E	-		5.772113
39	E	-		5.175224
40	E	-		5.551294
41	E	-		5.187755
42*	E	-		5.488117
43	E	-		5.173277
44	E	-		5.07263
45	E	-		4.980053
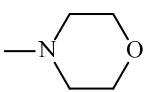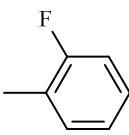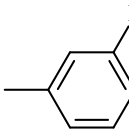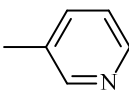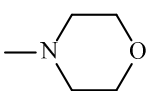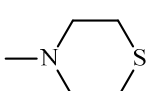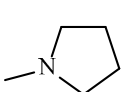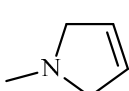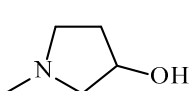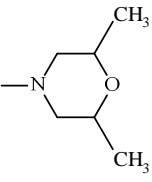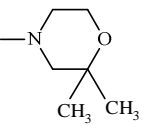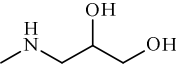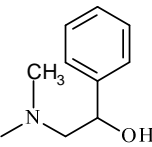
* Test set compounds

Computational work

Initially 2D structures of dataset compounds were drawn in Marvin application interface and after adding explicit hydrogen structures were converted in 3D. Further computational steps are depicted in fig. 2.
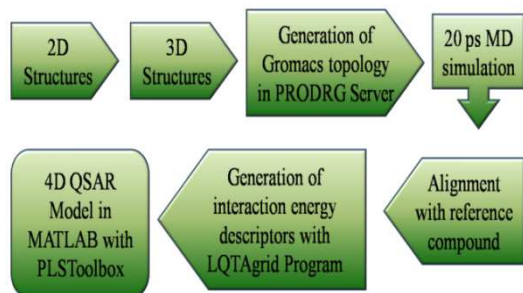
Fig. 2: Schematic representation of 4D-QSAR Methodology

Gromacs coordinates and topology files

The 3D structures were processed in PRODRG2 server [30] to generate coordinate and topology files of all the compounds from dataset. As the structures were not pre optimized, energy minimization option in PRODRG was chosen.

Wherever necessary, add hydrogen or hybridization patch was used during generation of coordinate and topology files. The charges generated in topology files by PRODRG server were manually replaced by gasteiger charges computed in UCSF chimera.
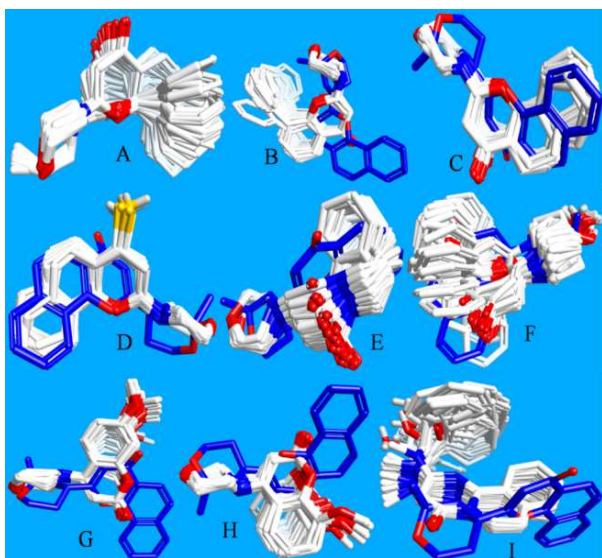
Fig. 3: 3 Alignment of conformers generated during MD simulation (CEP) (A) Aligned CEP of most active (reference) compound 22; (B) CEP of active compound 1 aligned with compound 22 (compound 22 shown blue colour); (C) CEP of active compound 2; (D) CEP of active compound 3; (E) CEP of active compound 12; (F) CEP of less active compound 21; (G) CEP of least active compound 30; (H) CEP of less active compound 31; (I) CEP of less active compound 45

Molecular dynamics simulation

Molecular Dynamics simulation was carried out in Gromacs 4.6.3. During MD simulation, GROMOS96 ffG43a1 force field was used in an explicit water model in a cubic box of 1A0 volume. MD simulation included heating the system at 50, 100, 200 and 350K for 20

picoseconds (ps) simulation time with 1 famto seconds (fs) step size. Long-range electrostatics and Van der waal interaction energies were calculated with a cut off radius of 1 Å with Particle Mesh Ewald (PME) method. Compound and solvent water was separately coupled. Parrinello-Rahman coupling and velocity rescaling thermostat (V-rescale) respectively controlled the pressure and temperature of the system. The system was then cooled down to 300 K. The trajectory generated was recorded at every 2 ps simulation time.

Alignment

The most active compound from dataset (Compound 22) was chosen as reference compound. Conformations of all other compounds generated during MD simulation were aligned to this reference compound. The alignments of conformers of the few most active (1, 2, 3 & 12) and least active compounds (21, 30 & 45) from dataset aligned with conformer of most active compound 22 are shown in fig. 3.

Descriptors of interaction energy

In order to generate interaction energy descriptors, grid box of size 14 x 14 x 14, large enough to accommodate the CEPs was used in LQTAgrid module. LQTAgrid uses hypothetical N-terminal of the protein as $-NH_3+$ probe to generate the matrix of interaction energy descriptors. The electrostatic property in terms of Coulombic potential function and steric 3D property in terms of Lennard-Jones potential function was generated as a descriptor matrix of 5488 descriptors containing 2744 Leenard-Jones and 2744 Coulombic potential based descriptors.

Variable selection and model development

Descriptor matrix was refined by eliminating descriptors having correlation lower than 0.3 leaving 523 descriptors. The data set was split into training set of 34 compounds and test set of 11 compounds. Test set compounds included the highest and lowest activity as well as structural diversity. The Partial Least square model was built using PLSToolbox ((Eigenvector Research, Inc) in MATLAB workspace. The model built by using absolute values, 10 latent variables and venetian blinds with 6 splits which includes 1 sample per split was found to be the best model.

RESULTS AND DISCUSSION

4 D QSAR Model

The objective of the current work was to build the best 4D-QSAR model with good predictive abilities and subsequently to exploit the 4D QSAR model in designing new DNA-PK / PI 3-K inhibitors. The approach of MD simulation and the consequent generation of interaction energy contributions with the aid of hypothetical $-NH_3+$ probe emulate interaction of important residues at the binding site of DNA-PK with compounds under investigation. Among many chemometric tools, multiple linear regression (MLR) and partial least square regression (PLS) are frequently used regression approaches in development of QSAR models. In current work as the number of refined descriptors was 523, MLR was not chosen. This is because the number of independent variable matrix exceeds the dependent variable vector, and generated model could have the over fitting. Partial least square regression (PLS) can be good in this situation and in current investigation PLS regression was carried out.

The data was split into 34 training set compounds and 11 test set compounds. In MATLAB workspace with PLS Toolbox, data was pre-processed by auto scaling the raw data. Venetian blind cross validation method with 5 number of sample splits with 1 sample per split was chosen. The model was built with 19 latent variables.

This PLS model showed R^2 calculated for training set 0.834502, root mean square error 0.188741, root mean square error predicted 0.575649, prediction bias -0.0221941. The pIC50 predicted with the residuals are shown in table 2. The plots of predicted activity against measured activity is shown in Fig. 4. Coefficient of most contributing descriptors is given in table 3.

Table 2: The measured pIC50 values and predicted pIC50 values for test set and training set compounds along with residuals

| Comp.	Measured pIC50	Predicted pIC50	Residuals
1	5.83268	5.75303	0.07964
2	6.63827	6.71624	-0.07796
3	6.58502	5.99735	0.58766
4	5.86012	5.97798	-0.11786
5*	6.44369	5.87118	0.57250
6	6.40893	6.17532	0.23360
7	5.90308	6.10552	-0.20243
8	5.48945	5.62230	-0.13285
9	5.28819	5.51838	-0.23019
10*	5.17652	5.52461	-0.34808
11	5.72124	5.34853	0.37271
12*	6.55284	5.37326	1.17957
13	5.89962	5.81422	0.08540
14*	5.78251	5.79515	-0.01263
15	6.02227	5.91948	0.10279
16*	5.92081	4.58487	1.33594
17	5.64975	5.65963	-0.00988
18	5.33068	5.33233	-0.00164
19	5.79317	5.81486	-0.02168
20	5.49620	5.88143	-0.38522
21*	5.03292	5.88427	-0.85135
22	6.72124	6.72132	-0.00012
23	5.38299	5.23753	0.14546
24	5.45345	5.55418	-0.10072
25	5.31695	5.37888	-0.06193
26*	5.05502	5.82225	-0.76723
27	5.27164	5.46657	-0.19493
28	5.09420	4.94749	0.14671
29	5.75696	5.49072	0.26623
30	4.94653	5.27887	-0.33233
31*	4.96098	5.51927	-0.55829
32	5.48545	5.41195	0.07350
33*	5.30277	4.88430	0.41846
34	5.06600	5.06552	0.00048
35	5.24336	5.24761	-0.00425
36	5.71669	5.71042	0.00626
37*	5.69897	5.77046	-0.07149
38	5.77211	5.45695	0.31516
39	5.17522	5.19812	-0.02290
40	5.55129	5.50205	0.04924
41	5.18775	5.50870	-0.32095
42*	5.48811	5.56078	-0.07266
43	5.17327	5.42157	-0.24829
44	5.07262	5.07059	0.00203
45	4.98005	4.98082	-0.00076

* Test set compounds
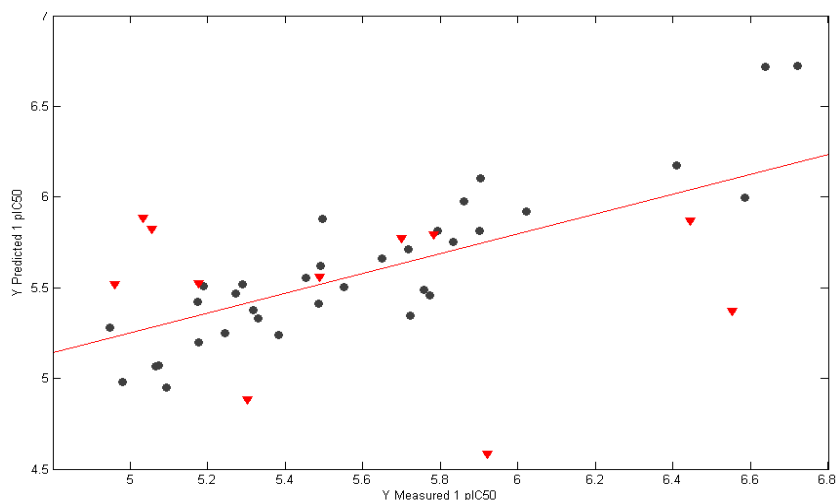
Fig. 4: Predicted pIC50 values against measured pIC50 values for training set and test set compounds (Black circles: training set compounds; red triangles: test set compounds)

Table 3: Contributions of descriptors (Variables) in final model

Variable	Coefficient	Variable	Coefficient
0_0_0_NH3+_LJ	34.704	0_0_1_NH3+_LJ	25.739
0_1_0_NH3+_LJ	23.749	0_0_2_NH3+_LJ	19.310
1_0_1_NH3+_LJ	17.505	0_1_1_NH3+_LJ	17.135
2_0_0_NH3+_LJ	17.087	0_2_0_NH3+_LJ	15.843
1_1_0_NH3+_LJ	15.478	5_0_0_NH3+_LJ	14.856
0_0_3_NH3+_LJ	14.603	1_0_2_NH3+_LJ	12.728
0_1_2_NH3+_LJ	12.629	3_0_0_NH3+_LJ	12.044
2_0_1_NH3+_LJ	11.742	6_0_0_NH3+_LJ	11.370
0_2_1_NH3+_LJ	10.997	0_0_4_NH3+_LJ	10.964
1_1_1_NH3+_LJ	10.563	0_3_0_NH3+_LJ	10.156
0_10_0_NH3+_LJ	-10.513	2_0_8_NH3+_LJ	-12.601
0_1_9_NH3+_LJ	-26.958	1_0_9_NH3+_LJ	-38.509
0_0_9_NH3+_LJ	-54.750		

The 4D-QSAR model showed that only Leenard-Jones (LJ) interaction energy descriptors are contributing to the model. LJ interaction energy descriptors showed importance of steric 3D features required in the compounds. Few LJ descriptors show negative contributions which revealed unfavourable region in the molecules which can affect the pIC50 adversely. More importantly the LJ descriptors around aromatic ring are inversely contributing to the model where as LJ descriptors around morpholine ring are favourable for the activity. This is in good agreement with the SAR proposed by Griffin RJ et al [25]. In line with these findings currently we are developing library of 2, 3 di substituted chromenones. The contributions of descriptors 0_0_0_NH3+_LJ, 0_0_1_ NH3+_LJ, 0_1_0_ NH3+_LJ, 0_0_2_ NH3+_LJ, 2_0_8_ NH3+_LJ, 0_1_9_NH3+_LJ, 1_0_9_NH3+_LJ, 0_0_9_ NH3+_LJ around most active compound 22 and least active compound 30 is shown in fig. 5.
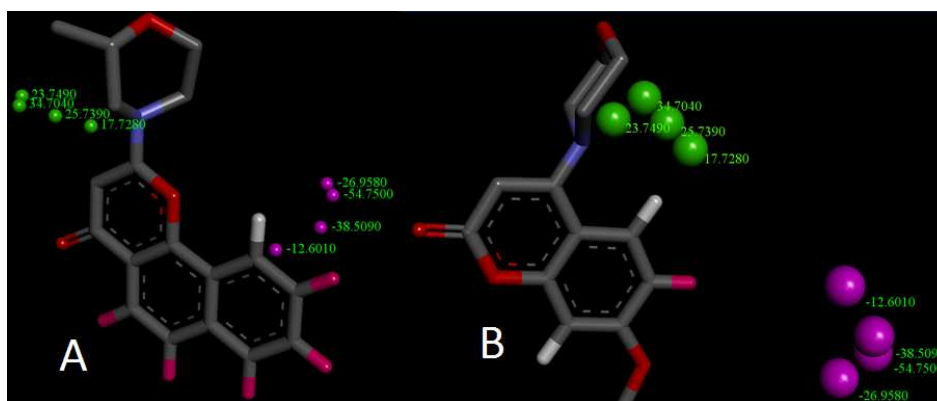

Fig. 5: Interpretation of interaction energy descriptors. (A) Interaction energy descriptors around most active compound 22; (B) interaction energy descriptors around least active compound 30

CONCLUSION

4D-QSAR model was built using gromacs based molecular dynamics simulation on chromoneone derivatives as DNK-PK inhibitors. In the model, interaction energy descriptors were constructed on CEP of each compound. PLS regression was carried out on selected descriptor matrix of 523 descriptors. The selected model with 19 latent variables showed R^2 calculated for training set 0.834502, root mean square error 0.188741, root mean square error predicted 0.575649, prediction bias -0.0221941 suggesting reasonable predictive abilities in the model developed. Few LJ interactions are important for higher activity of these compounds. As a part of future work, we are designing 2, 3 di substituted chromenones which will mainly contribute to LJ interactions.

CONFLICT OF INTERESTS

Declared None

REFERENCES

1. Abbas S, Radineh M, Omidreza F, Savis M, Ahmad R, Ramin M. Synthesis and cytotoxic activity of novel benzopyrano[3,2-c]chromene-6,8-dione derivatives. Med Chem Res 2011;20:466-74.
2. Reddy RK, Rao SP, Dev JG, Poornachandra Y, Ganesh Kumar C, Rao SP, *et al.* Synthesis of novel 1,2,3-triazole/isoxazole functionalized 2H-Chromene derivatives and their cytotoxic activity. Bioorg Med Chem Lett 2014;24(7):1661-3.
3. Gourdeau H, Leblond L, Hamelin B, Desputeau C, Dong K, Kianicka I, *et al.* Antivascular and antitumor evaluation of 2-amino-4-(3-bromo-4,5-dimethoxy-phenyl)-3-cyano-4H-chromenes, a novel series of anticancer agents. Mol Cancer Ther 2004;3:1375-84.
4. Mladenovic M, Vukovic N, Sukdolak S, Solujic S. Design of novel 4-hydroxy-chromene-2-one derivatives as antimicrobial agents. Mol 2010;15:4294-08.
5. Serbetci T, Birteksoz S, Prado S, Michel S, Tillequin F. Synthesis and antimicrobial activities of some sulphur containing chromene derivatives. Nat Prod Commun 2012;7(7):891-4.
6. Fadda AA, Berghot MA, Amer FA, Badawy DS, Bayoumy NM. Synthesis and antioxidant and antitumor activity of novel pyridine, chromene, thiophene and thiazole derivatives. Arch Pharm (Weinheim) 2012;345(5):378-85.
7. Cheng JF, Ishikawa A, Ono Y, Arrhenius T, Nadzan A. Novel chromene derivatives as TNF-alpha inhibitors. Bioorg Med Chem Lett 2003;3(13 Suppl 21):3647-50.
8. Ali TA, Abdel-Aziz SA, El-Shaaer HM, Hanafy FI, El-Fauomy AZ. Synthesis of some new 4-oxo-4H-chromene derivatives bearing

nitrogen heterocyclic systems as antifungal agents. Turk J Chem 2008;32:365-74.

9. Zghab I, Trimeche B, Mansour M, Hassine M, Touboul D, Jannet H. Regiospecific synthesis, antibacterial and anticoagulant activities of novel isoxazoline chromene derivatives. Arabian J Chem Forthcoming 2013; [Article in Press]

10. Drug Bank version 4.1 [Internet]. Drug bank: open data drug and drug target Database; Available from: http://www.drugbank.ca/drugs/DB01148. html

11. Nardi D, Leonardi A, Pennini R, Tajana A, Cazzulani P, Testa R. New basic esters of 2-phenyl-3-methyl-4-oxo-4H-1-benzopyran-8-carboxylic acid endowed with spasmolytic properties. Synthesis and pharmacological pharmacokinetic evaluation. Arzneimittelforsch 1993;43(1):28-34.

12. Sun W, Cama LD, Birzin ET, Warrier S, Locco L, Mosley R, *et al*. 6H-Benzo[c]chromen-6-one derivatives as selective ER beta agonists. Bioorg Med Chem Lett 2006;16(6):1468-72.

13. Hussain MK, Ansari MI, Yadav N, Gupta PK, Gupta AK, Saxena R, *et al.* Design and synthesis of ERa/ERb selective coumarin and chromene derivatives as potential anti-breast cancer and anti-osteoporotic agents. RSC Adv 2014;4:8828-45.

14. Mori J, Iwashima M, Takeuchi M, Saito H. A synthetic study on antiviral and antioxidative chromene derivative. Chem Pharm Bull 2006;54(3):391-6.

15. Naga Sudha B, Sridhara C, Girija Sastry C, Reddy YSR, Sreevidya O, Lavanya S, *et al*. Synthesis, characterisation and anthelmintic activity of 3-(4-acetyl-5-phenyl-4,5-dihydro-1,3,4-oxadiazol-2-yl)-2H-chromen-2-one derivatives. Indian J Chem 2013;52B:422-7.

16. Bhavsar D, Trivedi J, Parekh S, Savant M, Thakrar S, Bavishi A, *et al*. Synthesis and *in vitro* anti-HIV activity of N-1,3-benzo[d]thiazol-2-yl-2-(2-oxo-2H-chromen-4-yl)acetamide derivatives using MTT method. Bioorg Med Chem Lett 2011;21(11):3443-6.

17. Mungra DC, Patel MP, Rajani DP, Patel RG. Synthesis and identification of ß-aryloxyquinolines and their pyrano[3,2-c]chromene derivatives as a new class of antimicrobial and antituberculosis agents. Eur J Med Chem 2011;46(9):4192-00.

18. Vijaya Kumar P, Rajeswar Rao V. Synthesis and antitubercular,antiviral and anticancer activity of 3-(3-mercaptoalkyl-7H-[1,2,4]triazolo[3,4-b][1,3,4]-thiadiazin-6-yl)chromen-2-one and its derivatives. Indian J Chem 2008;47B:106-11.

19. Chen JJ, Wang TY, Hwang TL. Neolignans, a coumarinolignan, lignan derivatives, and a chromene: anti-inflammatory constituents from Zanthoxylum avicennae. J Nat Prod 2008;71(2):212-7.

20. Asrondkar Al, Patil VN, Mishra NU, Bobade AS, Chowdhary AS. Synthesis and study of (5Z)-5-[(4-oxo-4H-chromen-3-yl) methylidene]-1,3-thiazolidine-2,4-dione derivative. Der Pharm Chem 2013;5(4):288-92.

21. Bin L, Long-Guan X, Xiao-Hua X, Yong-Hong L. Synthesis, crystal structure and herbicidal activity of 3-benzoyl-4-hydroxycoumarin derivatives. Chin J Org Chem 2011;31(12):2067-73.

22. Sivakumar KK, Rajasekaran A. Synthesis, *in vivo* analgesic and *in vitro* anti-microbial activity of 3-amino-4-[2-(substituted phenyl)hydrazin-1-ylidene]-1-[(2-oxo-2H-chromen-3-yl)carbonyl]-4,5-dihydro-1H-pyrazol-5-one and its schiff bases. Int J Res Pharm Chem 2014;4(3):517-27.

23. Hegab MI, Abdulla MM. 4-Chloro-2,2-disubstituted chromen-3-carboxaldehyde: synthesis of some fused polycyclic heterocycles as anti-inflammatory, analgesic, anticonvulsant, and antiparkinsonian agents. Arch Pharm (Weinheim) 2006;339(1):41-7.

24. Ronad PM, Maddi VS, Koti BC, Kurhe YV, Swamy A, Swamy Ahmt, *et al*. Evaluation of anticonvulsant activity of novel series of benzopyran-2-one derivatives by PTZ induced seizure model in mice. Indian J Novel Drug Delivery 2010;2(4):158-61.

25. Griffin RJ, Fontana G, Golding BT, Guiard S, Hardcastle IR, Leahy, *et al.* Selective benzopyranone and pyrimido[2,1-a]isoquinilin-4one inhibitors of DNA-dependent protein kinase: synthesis, structure activity studies and radiosensitization of a human tumor cell line *in vitro*. J Med Chem 2005;48:569-85.

26. Winkler DA. The role of quantitative structure activity relationship (QSAR) in biomolecular discovery. Briefings Bioinf 2002;3(1):73-86.

27. Hopfinger A, Wang S, Tokarski J, Jin B, Albuquerque M, Madhav P, *et al*. Construction of 3D-QSAR models using the 4D-QSAR analysis formalism. J Am Chem Soc 1997;119:10509-24.

28. Martins JPA, Barbosa EG, Pasqualoto KFM, Ferreira MMC. LQTA-QSAR: a new 4D-QSAR methodology. J Chem Inf Model 2009;49:1428-36.

29. Morris GM, Huey R, Lindstrom W, Sanner MF, Belew RK, Goodsell DS, *et al*. Autodock4 and autodock tools 4: automated docking with selective receptor flexiblity. J Comput Chem 2009;16:2785-91.

30. Schuttelkopf AW, van Aalten DMF. PRODRG: a tool for high-throughput crystallography of protein-ligand complexes. Acta Crystallogr 2004;D60:1355-63.